Electron-impact excitation from the ground and the metastable levels of Ar I

Arati Dasgupta,[1] M. Blaha,[2] and J. L. Giuliani[1]
[1]*Radiation Hydrodynamics Branch, Plasma Physics Division, Naval Research Laboratory, Washington, D.C. 20375*
[2]*Berkeley Scholars, Springfield, Virginia 22151*
(Received 27 July 1999; published 9 December 1999)

Electron-impact excitation of Ar I from the ground $3p^6\,{}^1S_0$ as well as the two metastable levels of the $3p^5 4s$ ($^3P_2$ and $^3P_0$) configuration to all ten levels of the $3p^5 4p$ excited configuration are calculated in the distorted-wave approximation. Polarization of the ground state is explicitly included by adding a polarization potential in the calculation. Unitarization of the scattering matrix **S** is carried out by including the elastic terms, and effects of unitarization in the LS as well as jj formalisms are investigated. The excitation cross sections are calculated from threshold to ~100 eV. The calculations are compared and contrasted with recent experimental data and other theoretical work. The study shows that the effect of the polarization potential is not very significant but unitarization of the **S** matrix reduces the cross sections considerably and the cross sections obtained using the two different methods of unitarization are significantly different for some excitation transitions. The results are useful for analyzing low-pressure plasmas used in processing applications as well as electron beam excitation, as in excimer lasers.

PACS number(s): 34.80.Dp, 34.50.Fa

I. INTRODUCTION

Electron-impact excitation of the ground and metastable levels of argon is not only of interest for an understanding of the basic physics of atomic collision processes, but also for the variety of applications in gaseous electronics. Coburn and Chen [1] first pointed out that optical emission spectroscopy of a discharge plasma with a known concentration of an inert gas, such as argon, can be used to determine the concentration of reactive species, such as atomic fluorine. In the simplest version of optical actinometry, the coronal equilibrium approximation is adopted, wherein the excitation rates of Ar and F from the ground levels to those responsible for the emission is known from atomic physics, and combined with observed intensities to evaluate the relative concentration of fluorine to argon. Savas [2] noted that measurements from a low-pressure discharge were not consistent with direct excitation of the argon from the ground level, and suggested that excitation of long-lived metastable argon atoms was also an important process for interpreting the data. Multispecies actinometry with several noble gases can also be used to estimate the electron temperature, as long as the excitation from the ground and metastable levels is known [3]. In higher pressure discharges, ~1 Torr, with higher electron densities both excitation and de-excitation must be accounted for in a collisional-radiative equilibrium model to determine the dissociation fraction of nitrogen through optical actinometry [4]. In addition to the interest in excitation of argon by low-energy electrons (~1 eV) in plasma processing, high-energy electron beams (~500 keV) are used to pump the amplifier cell in krypton fluoride lasers [5]. The cell generally contains ~50% argon buffer because the three-body quenching of the excited excimer KrF* by collisions with argon is significantly less than with krypton [6]. Cross sections for ionization and excitation of argon (and krypton) by energetic electrons are essential for determining the slowing down of the electron beam in the laser cell [7]. The secondaries resulting from the interactions eventually degrade and form a background distribution of electrons in the cell with a mean energy of a few eV. This nascent population of electrons can also pump the argon buffer gas, and must be accounted for in kinetic models of the amplifier [8]. It is thus useful to have collisional excitation and ionization cross sections over a broad energy range to model electron interactions in plasma discharges.

In this work, we present detailed calculations of the integral excitation cross sections to the all ten levels of the $3p^5 4p$ configuration from the two $J=1$ metastable levels of $3p^5 4s$ configuration of neutral argon, as well as the excitation cross sections from the ground to all the excited levels of $3p^5 4s$ and $3p^5 4p$ configurations. There exist several calculations [9–15] and measurements [16–19] for excitation from the ground level $3p^6\,{}^1S_0$ to the four fine-structure levels $^3P_2$, $^3P_1$, $^3P_0$, and $^1P_1$ of $3p^5 4s$. For excitation to the fine-structure levels of the $3p^5 4p$ configuration from the ground level, there also exist a host of calculations [20–22,14,15] and experimental measurements [23–26]. *R*-matrix calculations of the integral excitation cross sections to all these levels were also calculated by Bartschat and Zeman [27]. However, available experimental or theoretical excitation cross sections from the metastable levels are very sparse. On the theoretical side there exist only average configuration Born cross sections by Hyman [28], and very recent *R*-matrix calculation by Bartschat and Zeman [29]. The experimental group at the University of Wisconsin has also recently measured most of these metastable excitation cross sections [30–32]. The experimental data from a Russian collaboration [33] present very different results than the results of the Wisconsin group. Since accurate knowledge of these metastable excitation cross sections are crucial for plasma modeling for discharges and laser applications, it therefore seems necessary to pursue further theoretical investigation of these important metastable excitation to compare with experimental data, and to compare and complement the only available level-to-level theoretical calculation.

Even though there exist several calculations of excitation

cross sections from the ground state, the purpose of presenting our results for these cross sections are due to the following reasons, namely, (i) to verify the results of other distorted-wave (DW) calculations, (ii) to compare our DW results with other methods of calculations, and (iii) to complete the database for excitation to all levels of the $4s$ and $4p$ levels. Most of the above-mentioned theoretical calculations do not present excitation cross sections to all 14 excited states primarily due to lack of convergence near thresholds. In our approach we use *ab initio* wave functions with full electron exchange and polarization of the outermost electron and proper conversion of the **T** matrix from the **R** matrix and the cross sections converge in all cases. Although multistate *R*-matrix calculations are expected to be most reliable at low electron collision energies, the less complex DW calculations are more efficient, especially for high electron energies. In addition, the accuracy of *R*-matrix calculations is not as good at higher energies because of many open channels. This paper seeks modifications to the DW method which maintain efficiency while improving accuracy by including a polarization potential and proper unitarization.

In Sec. II the distorted-wave formalism and the computational details used in this work are described, and in Sec. III the results obtained in this calculation and comparisons with other calculations and experimental data are discussed, followed by a brief summary in Sec. IV.

II. THEORY AND CALCULATIONS

An energy-level diagram involving all the levels for this present calculation is shown in Fig. 1. In this figure we show the LS as well as the Paschen notations $1s_5$-$1s_2$ for the $3p^5 4s$ excited configuration and $2p_{10}$-$2p_1$ for the $3p^5 4p$ excited configuration. Since the argon atom does not conform to LS coupling and the electrostatic and spin-orbit interactions for this system are comparable, an intermediate coupling scheme is employed in this work. Spin-orbit interaction is dominated by the $3p^5$ core, and the spin-orbit parameter $\zeta_{3p}=0.0043$ a.u. is comparable to the electrostatic energy -0.016 a.u. of $3p^5 4p\ ^3P$, for example.

A. Bound states

The bound-state wave functions of the core $1s$, $2s$, $2p$, and $3s$ orbitals for this calculation were obtained by using the parameters given by Clementi and Roetti [34]. For the outermost $3p$ orbital and all excited bound states, we employed a semiempirical approximation [35]. The radial part of the bound wave function P_{nl} in this method is obtained by solving the equation

$$\left[\frac{d^2}{dr^2}-\frac{l(l+1)}{r^2}-2V_o(r)-2\beta V_{ex}(r)-2E\right]P_{nl} = -\mu_{n'l}P_{n'l}, \tag{1}$$

where V_0 and V_{ex} are the Coulomb and static exchange potentials. E is the experimental ionization energy of the electron, the parameter β is adjusted to ensure the correct asymptotic behavior of P_{nl}, and $\mu_{n'l}P_{n'l}$ on the right-hand side of the Eq. (1) is also adjusted to make it orthogonal to other bound orbitals of the same angular momentum l. Atomic units are used throughout in any expression or equation.

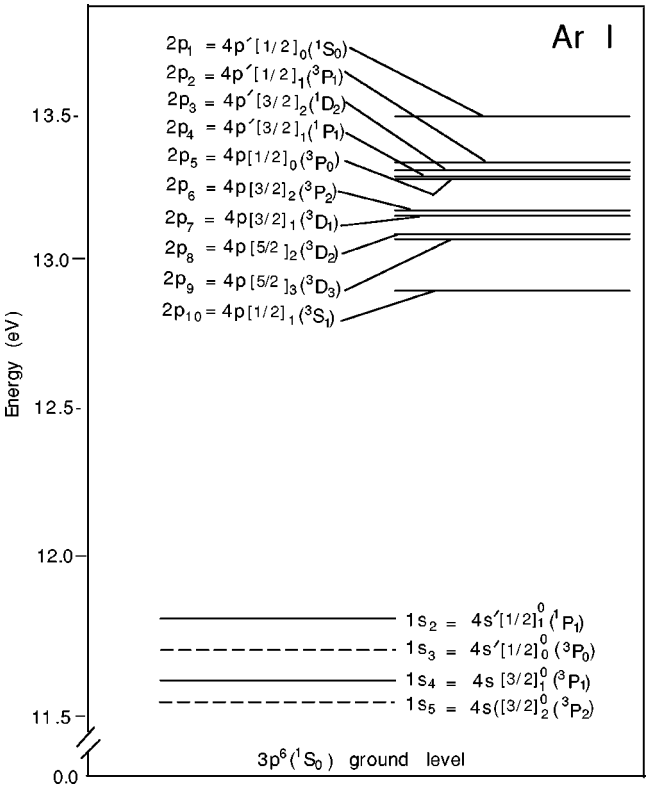

FIG. 1. Energy-level diagram showing the $3p^5 4s$ ($1s_2$-$1s_5$) and $3p^5 4p$ ($2p_1$-$2p_{10}$) levels of Ar I. The dashed lines show the two metastable levels $1s_5$ and $1s_3$.

Even though this method is similar to the Hartree-Fock-Slater (HFS) procedure, in this approach the contribution of P_{nl} in the expression for V_0 and V_{ex} is not included. This omission not only simplifies the calculation, but also automatically leads to the correct asymptotic form of the potential V_0. In the HFS procedure, the constant E is determined by using a variational approach by the solution of the radial equation, whereas we use experimental ionization energy for E and vary β. This method emphasizes the behavior of the outer part of P_{nl} which is important for collision calculations, and, unlike the HFS method, the orthogonality of wave functions with the same l has to be done explicitly in this method. This orthogonalization is very important for monopole excitations.

The radial wave functions for the four $3p^5 4s$ levels $1s_5$, $1s_4$, $1s_3$, and $1s_2$, and the ten $3p^5 4p$ levels $2p_{10}$, $2p_9$, $2p_8$, $2p_7$, $2p_6$, $2p_5$, $2p_4$, $2p_3$, $2p_3$, and $2p_1$ are calculated by using the experimental threshold energy for each fine-structure level. Thus, for each level, we calculate the F and G integrals and the spin-orbit parameter ζ_{nl}. In the calculation using intermediate coupling approximation each mixed level for a given angular momentum J is expressed as

$$|\alpha J\rangle = \sum_{SL} C_{\alpha SLJ}|\alpha SLJ\rangle, \tag{2}$$

TABLE I. Mixing coefficients for the excited levels of $3p^5 4s$ and $3p^5 4p$ configurations.

Level	Paschen notation	J	E (eV)	Mixing coefficients
$4s[3/2]_2^o\ ^3P_2$	$1s_5$	2	11.548	$^3P_2$
$4s[3/2]_1^o\ ^3P_1$	$1s_4$	1	11.624	$0.9104\ ^3P_1+0.4137\ ^1P_1$
$4s'[1/2]_0^o\ ^3P_0$	$1s_3$	0	11.723	$^3P_0$
$4s'[1/2]_1^o\ ^1P_1$	$1s_2$	1	11.828	$0.9104\ ^1P_1-0.4137\ ^3P_1$
$4p[1/2]_1\ ^3S_1$	$2p_{10}$	1	12.906	$0.4742\ ^3D_1+0.1871\ ^3P_1+0.1172\ ^1P_1+0.9753\ ^3S_1$
$4p[5/2]_3\ ^3D_3$	$2p_9$	3	13.076	$^3D_3$
$4p[5/2]_2\ ^3D_2$	$2p_8$	2	13.093	$0.8162\ ^3D_2-0.5503\ ^1D_2+0.1760\ ^3P_2$
$4p[3/2]_1\ ^3D_1$	$2p_7$	1	13.153	$0.7115\ ^3D_1+0.4121\ ^3P_1-0.5690\ ^1P_1-0.1418\ ^3S_1$
$4p[3/2]_2\ ^3P_2$	$2p_6$	2	13.172	$0.2280\ ^3D_2+0.5866\ ^1D_2+0.7710\ ^3P_2$
$4p[1/2]_0\ ^3P_0$	$2p_5$	0	13.274	$0.9393\ ^3P_0-0.3429\ ^1S_0$
$4p'[3/2]_1\ ^1P_1$	$2p_4$	1	13.283	$0.7021\ ^3D_1-0.3859\ ^3P_1+0.5984\ ^1P_1-0.0012\ ^3S_1$
$4p'[3/2]_2\ ^1D_2$	$2p_3$	2	13.302	$0.5309\ ^3D_2+0.5941\ ^1D_2-0.6043\ ^3P_2$
$4p'[1/2]_1\ ^3P_1$	$2p_2$	1	13.328	$0.2878\ ^3D_1-0.8038\ ^3P_1-0.5518\ ^1P_1+0.2204\ ^3S_1$
$4p'[1/2]_0\ ^1S_0$	$2p_1$	0	13.480	$0.3430\ ^3P_0+0.9393\ ^1S_0$

within the same configuration α. The mixing coefficients $C_{\alpha SLJ}$ are then obtained by diagonalizing the Hamiltonian with level-specific F, G, and ζ_{nl} for each J. Table I lists these mixing coefficients. The LS coupling designations in Table I correspond to the dominant LS level in the expansion for each level, and these designations as well as the mixing coefficients are in agreement with the predictions of Madison *et al.* [14]. In our calculation, the $4p$ radial functions are made orthogonal to the $3p$ wave function.

B. Continuum states

The radial part of the scattering wave function F_{kl} used for the calculation of elements of the reactance matrix **R** is generated in the DW method by solving the equation

$$\left[\frac{d^2}{dr^2}-\frac{l(l+1)}{r^2}-2V_0(r)-2V_{ex}(r)-2V_p+k^2\right]F_{kl} = -\sum_n \mu_{nl}P_{nl}(r), \tag{3}$$

where the polarization potential V_p is the distortion of the atom by the colliding electron at large distance. The polarization potential V_p, which behaves as $-\alpha/r^4$ for $r\to\infty$ where α is the polarizability of the atom, is calculated in the polarized orbital method. The experimental polarizability $\alpha = 11.06a_0^3$ was used to estimate V_p at very large distances. A detailed description of the method and calculation of this potential was given by Dasgupta and Bhatia [36]. This method is appropriate for low-energy collisions when the colliding electron velocity is small compared to that of the atomic electrons, and first-order perturbation theory is used for the distortion. At large distances, the colliding electron produces a dipole moment in the atom and the electron then moves in an induced dipole potential V_p. Only the dipole part of this interaction is included in deriving V_p. In our calculation we have included polarization due only to the outer $3p$ orbital. For excitation from the ground state, this approximation is reasonable, but for excitation from the metastable states one should properly include the polarization due to the excited orbitals. The polarization potential calculated using the perturbed $3p$ orbitals is shown in Fig. 2.

The scattering wave function is calculated using a distorted potential, and electron exchange contributions are included in the calculation of the reactance matrix **R**. The wave function F_{kl} is made orthogonal to all P_{nl} with same angular momentum l by varying μ_{nl} in Eq. (3). The effect of core exchange in the potential was found to be small, and was therefore neglected. Up to 100 partial waves were included for the calculations of both direct and exchange amplitudes. Distorted waves were calculated using static potential obtained from the charge densities of the final states for both input and output channels, as experience shows that it gives the best results [11]. We have not included any rela-

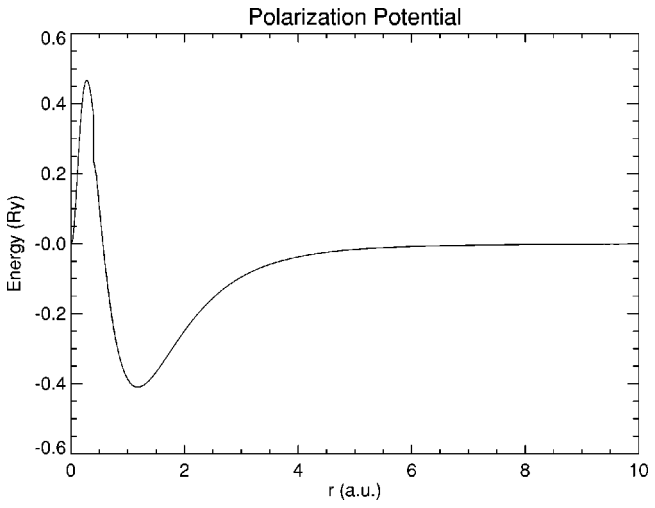

FIG. 2. Polarization potential V_p as a function of distance. This potential was obtained using only the perturbation of the outer $3p$ orbital.

tivistic effect in our calculation, since it was found to be negligible for the integrated cross sections published by Madison *et al.* in Ref. [14].

C. Excitation cross sections

The elements of the reactance matrix **R** are calculated first from the variational expression using our bound and continuum wave functions, and then the elements of the transmission matrix **T** and scattering matrix **S** are obtained using the well-known relationship given by

$$\mathbf{S}=\mathbf{1}-\mathbf{T}=\frac{(i+\mathbf{R})}{(i-\mathbf{R})}. \tag{4}$$

If the **R** matrix is calculated using an approximate method, then the **S** matrix obtained from Eq. (4) is unitary, but if the **S** matrix is calculated directly using first-order perturbation, the condition for unitarity may not be satisfied. For large cross sections of metastable excitations, this unitarizations, which guarantees conservation of flux of incoming and outgoing particles, is very important [37].

Collision strengths and equivalently cross sections for a transition between fine-structure levels αSLJ and $\alpha' S' L' J'$ are obtained by calculating the $T(\alpha SLJ,\alpha' S' L' J')$ matrices, which are obtained from the $T(\alpha SL,\alpha' S' L')$ matrices using the transformation

$$\begin{aligned}T(\alpha SLJlj&J^T,\alpha' S' L' J' l' j' J^T)\\ &=\sum_{S^T L^T} C\left(\frac{1}{2}lj,SLJ,S^T L^T J^T\right)\\ &\quad\times T(\alpha SLlS^T L^T,\alpha' S' L' l' S^T L^T)\\ &\quad\times C\left(\frac{1}{2}l' j',S' L' J',S^T L^T J^T\right),\end{aligned} \tag{5}$$

where the recoupling coefficient C is given by

$$\begin{aligned}C&\left(\frac{1}{2}lj,SLJ,S^T L^T J^T\right)\\ &=[(2S^T+1)(2L^T+1)(2J+1)(2j+1)]^{1/2}\\ &\quad\times X\left(\frac{1}{2}lj,SLJ,S^T L^T J^T\right),\end{aligned} \tag{6}$$

and $X(abc,def,ghi)$ are 9-j symbols. The collision cross sections **Q** for transition αSLJ-$\alpha' S' L' J'$ is given by

$$\begin{aligned}Q(\alpha SLJ,&\alpha' S' L' J')\\ &=\frac{\pi k^{-2}}{2(2J+1)}\sum_{ll' jj' J^T}(2J^T+1)\\ &\quad\times|T(\alpha SLJljJ^T;\alpha' S' L' J' l' j' J^T)|^2.\end{aligned} \tag{7}$$

By applying this transformation given by Eq. (5) to the **T** matrices (characterized by $S^T L^T$), we tacitly assume that during the collision the spin-orbit coupling of atomic electrons is weak, and the atom behaves as if it were temporarily in pure LS states and only recoupled to form SLJ states after the collision. If, however, this is not the case, and the SLJ states are well defined even during the collision, then it would be more proper to apply the transformation [Eq. (5)] directly to **R** matrices and only then use Eq. (4) to obtain **T** (characterized by J^T) and unitarized **S** matrices. Collision strengths or cross sections obtained from the two alternatives are generally different. In our calculation we have adopted the first alternative, i.e., unitarization before transformation [Eq. (5)]. The reason for choosing this method of unitarization is mainly because it is simpler. However, we have calculated the cross sections using the alternative method of unitarization of the J^T matrices for several transitions, and compared the results as discussed below. We have also included elastic terms in the unitarization of the **S** matrix.

To obtain the collision strengths $\Omega(\alpha J,\alpha' J')$ or cross sections $Q(\alpha J,\alpha' J')$, we first calculate all possible $R(\alpha SLlS^T L^T,\alpha' S' L' l' S^T L^T)$ involved in the αJ-$\alpha' J'$ transition, obtain **T** using Eq. (4) for all combinations αSL, and $\alpha' S' L'$, and then perform transformation [Eq. (5)].

The **T** matrix elements to be used in Eq. (7) to obtain the final cross sections $Q(\alpha J,\alpha' J')$ between mixed levels αJ and $\alpha' J'$ are given by

$$\begin{aligned}T(\alpha Jlj&J^T,\alpha' J' l' j' J^T)\\ &=\sum_{\substack{SL\\ S' L'}} C_{\alpha SL} C_{\alpha' S' L'} T(\alpha SLJljJ^T,\alpha' S' L' J' l' j' J^T).\end{aligned} \tag{8}$$

As in the case of transition between pure αSLJ and $\alpha' S' L' J'$ levels, even for mixed αJ and $\alpha' J'$ levels the other alternative for unitarization involve the transformation of the **R** matrix first according to Eq.(5); this is followed by a mixing of **R** matrices using Eq. (8), and one finally obtains **T** matrices and cross sections $Q(\alpha J,\alpha' J')$ using Eqs. (4) and (7).

III. RESULTS

A. Ground-state excitation

Excitation from the ground state to the $4s$ and $4p$ levels of neutral argon has been investigated quite extensively and is well documented in the published literature. In Fig. 3 we present our total cross section for the excitation of the $1s_5$, $1s_4$, $1s_3$, and $1s_2$ levels of the $3p^5 4s$ configuration. Of these levels, the $J=2$ $1s_5$ and $J=0$ $1s_3$ levels are true metastables and the other two $J=1$ mixed states are also long-lived. The dotted curve in this figure is the unpublished 41-state R-matrix calculation of Ref. [27] and the broken curve is the semirelativistic distorted-wave (SRDW) calculation of Ref. [14]. The solid circles are experimental data points of Ref. [18] using laser-induced fluorescence, and the triangles are the results from electron-loss measurements of Ref. [16]. Our cross sections for the $1s_5$ state agree quite well with the R-matrix predictions, whereas the SRDW results of Madison *et al.* are somewhat larger at low energy. There is also quite a good agreement between our results and the experimental

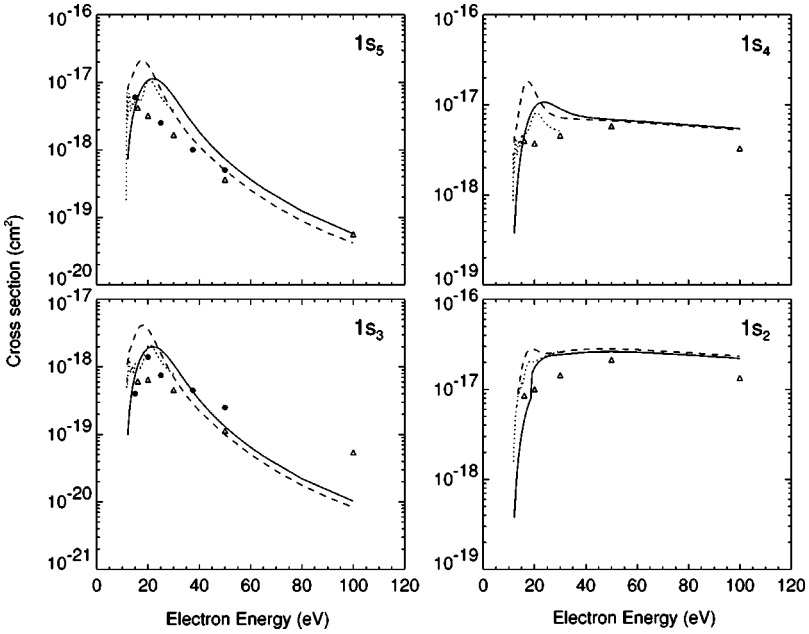

FIG. 3. Excitation cross sections from the ground to the $1s_2$-$1s_5$ excited levels of the $3p^5 4s$ configuration as a function of collision energy. The solid lines represent this calculation; dashed lines, SRDW results (Ref. [14]); dotted lines, *R*-matrix results (Ref. [27]); solid circles, experiment (Ref. [18]); triangles, experiment (Ref. [16]).

data, except that our cross sections are somewhat larger in the electron energy range of 20–40 eV. For the other metastable $1s_3$ level, we see very similar behavior, except that the experimental cross section of Ref. [16] at 100 eV is much larger than the theoretically predicted value. For the optically allowed $1s_2$ and $1s_4$ levels, our results and that of Madison *et al.* are usually higher than the experimental measurements of Chutjian and Cartwright [16]. There is reasonable agreement between our results and the *R*-matrix calculations for these levels but the SRDW calculation of Madison *et al.* [14] has sharp low-energy peaks, especially for the $1s_4$ level. Both our calculation and the *R*-matrix calculation show a much smaller peak for the $1s_4$ level. This peak disappears if we use a ground-state distorting potential instead of excited-state potential for both the initial- and final-state wave functions. Madison *et al.* also noticed the same behavior for their peaks.

In Fig. 4 we compare our excitation cross sections with other calculations and experimental data for the $2p_{10}$ through $2p_1$ levels of the $4p$ configuration. Our calculation is shown as a solid curve whereas the dashed and dash-dotted curves show the SRDW of Ref. [14] and another nonrelativistic distorted-wave (NRDW) result of Bubelev and Grum-Grzhimailo [21], respectively. Since our calculations are very similar to the NRDW calculations, it is not surprising that in most cases the two sets of cross sections are very close to each other. The dotted curve, which only goes up to 30 eV, is the unpublished 41-state *R*-matrix calculation of Bartschat and Zeman [27]. The triangles represent the experimental data of Chutjian and Cartwright [16], and the solid circles are recent experimental measurements of Chilton *et al* [26]. We group the discussion on the comparison according to the J value of the excited states.

It can be seen that our cross sections to the $J=3$ $2p_9$ level, which is the only pure LS-coupled state among all the ten levels in the $2p$ manifold, is in quite good agreement with the experimental data of Chilton *et al.* [26] except at the electron energy of 100 eV. All the theoretical cross sections are in close agreement, except that the SRDW cross sections of Madison *et al.* [14] are somewhat larger at lower energies. The theoretical cross sections for this level all fall off as E^{-3}, as they should, because this level is excited by a pure exchange transition. However the experimental data of Chilton *et al* [26] do not follow such energy dependence and fall off much slower.

All the theoretical cross sections for excitation to the $J=2$ states, $2p_8$, $2p_6$, and $2p_3$ are close to each other, except that the *R*-matrix results of Bartschat and Zeman for $2p_6$ are higher than the others. The SRDW results of Ref. [14] are given for energies above 25 eV. For all three transitions our calculations are very close to the measurements of Chutjian and Cartwright at high energies, and the measurements of Chilton *et al.* [26] are always larger. Since these levels have both direct and exchange contributions, the high-energy cross sections are dominated by the behavior of the $^1D_2$ direct state, and the falloff is much slower than the $J=3$ cross sections.

For the $J=1$ excitations, which involve $2p_{10}$, $2p_7$, $2p_4$, and $2p_2$ levels, there is very good agreement at high energies among all the theoretical calculations. At low energies, the theoretical calculation of Madison *et al.* are larger, whereas the *R*-matrix cross sections are in good agreement except that the cross sections for the $2p_{10}$ excitation are much lower. The disagreement of excitation cross sections at high energies between our calculations and measurements is most prominent for excitation to these $J=1$ $3p^5 4p$ levels from the ground, except for the excellent agreement with the experimental data of Chutjian and Cartwright [16] for the $2p_{10}$ level. Since these levels are all excited by exchange scattering because of angular momentum and parity selection rules, one would expect a much faster falloff than the experimental data show at higher energies. Although there is a slower falloff of the results of Ref. [16] compared to ours for these transitions, the cross sections measured by the Wisconsin

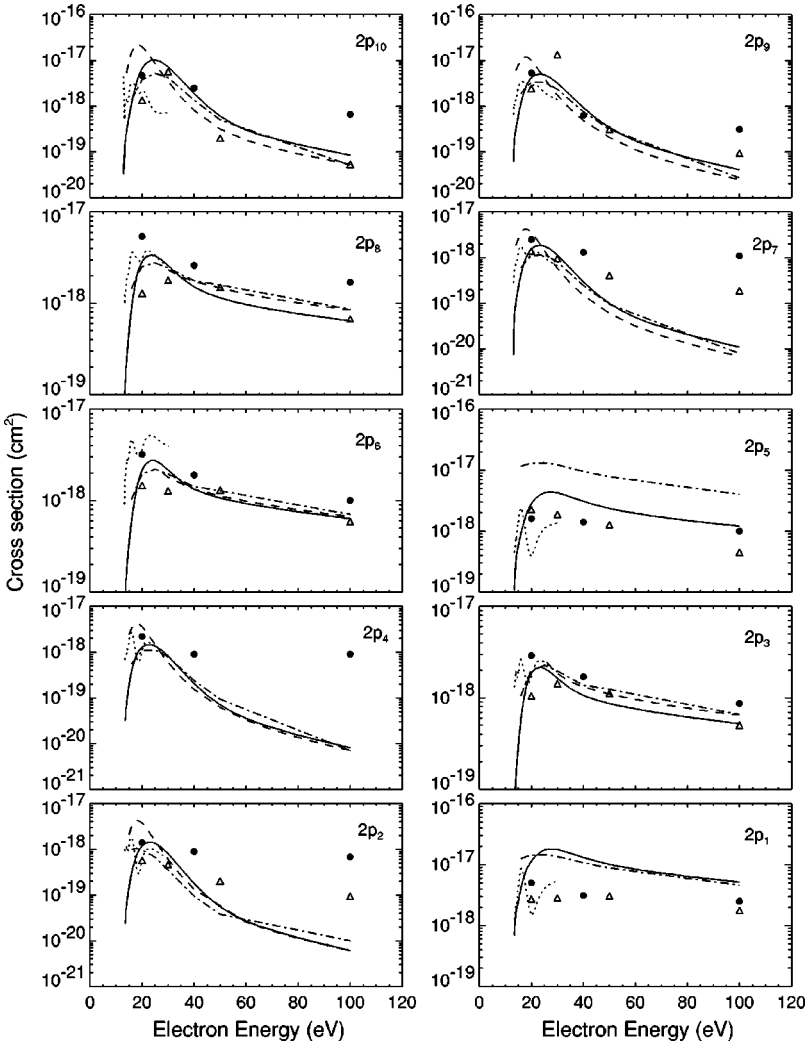

FIG. 4. Excitation cross sections from the ground to the $2p_1$-$2p_{10}$ excited levels of the $3p^5 4p$ configuration as a function of collision energy. The solid lines represent this calculation; dashed lines, SRDW results (Ref. [14]); dash-dotted lines, NRDW results (Ref. [21]); dotted lines, *R*-matrix (Ref. [27]); solid circles, experiment (Ref. [26]); triangles, experiment (Ref. [16]).

group are much larger and, except in the case of $2p_{10}$ excitation, they are almost flat at higher energies, and thus the disagreement with our results is more pronounced. One explanation for this could be that although excitation to these levels stems from exchange scattering, these levels could be excited by second-order transitions with two direct components. The second-order cross sections typically have a E^{-2} falloff. Thus for the apparent exchange transitions which can be attained by two direct excitations having dominant contributions at high energies, it becomes important to include these secondary levels. Inclusion of these second-order effects in the distorted wave formalism cannot be done very easily, and close-coupling calculations including these channels can give better results even at high energies for these cases. We notice that the disagreements between the cross sections of Chutjian and Cartwright [16] and the Wisconsin group are also greatest for these $J=1$ $3p^5 4p$ excitation from the ground at high energies. The very close agreement of our results with those of Chutjian and Cartwright at low energies for these transitions, and even at high energies for the $2p_{10}$ level (and also a much better agreement of our results at higher energies for the other three $J=1$ transitions, if we extrapolate our results using a E^{-2} dependence for secondary transitions), suggest that there may be some problems with the high-energy measurements of the Wisconsin group.

The cross sections for two $J=0$ levels $2p_5$ and $2p_1$ levels are also compared in this figure. Our present calculation for the $2p_5$ level shows very good agreement with the experimental data of Chilton *et al.* [26] at 100 eV. The NRDW calculation of Ref. [21] for this excitation is much larger, whereas the *R*-matrix calculation is much smaller than our results. For the $2p_1$ case, however, our cross sections are close to those of Ref. [21], and they are much larger than the experimental data as well as the *R*-matrix cross sections. For this monopole transition we find that it is very difficult to obtain cross sections which agree with experimental measurements for any collision involving either atoms or ions. Our earlier experience in calculating monopole excitation cross sections even for high-*Z* (nuclear charge) ions was similar. Specifically, for an investigation to predict x-ray lasing gain, the excitation cross section from the ground state $2p^6\,{}^1S_0$ to the $2p^5 3s\,{}^1S_0$ level of Se^{24+} were much larger than experimental findings [38].

B. Excitation from $1s_3$ excited metastable level

Recent *R*-matrix calculation by Bartschat and Zeman [29] have been performed for excitation from the $1s_3$ and $1s_5$

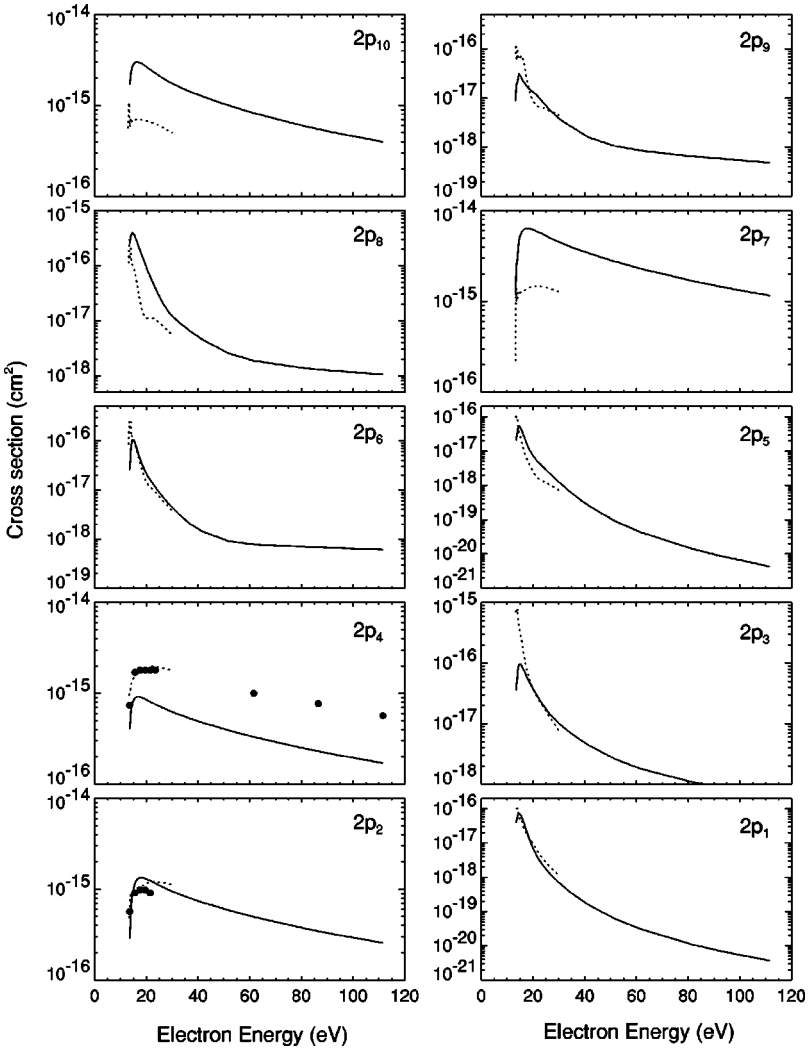

FIG. 5. Excitation cross sections from the $1s_3$ ($^3P_0$) to the $2p_1$-$2p_{10}$ excited levels of the $3p^5 4p$ configuration as a function of collision energy. The solid line represent this calculation; dotted lines, *R* matrix (Ref. [29]); solid circles, experiment (Refs. [31] and [32]).

levels. However, the cross sections are calculated for electron collision energies only up to 30 eV. Very recent experimental measurements [32] of excitation cross section from these metastable levels by the Wisconsin group presented data for high electron energies, supplementing their previously published results [31] for only a few energies near excitation threshold.

Results of our calculation for the excitation cross sections from the $1s_3$ level to all the $2p_1$-$2p_{10}$ levels are shown in Fig. 5. In this figure we compare our calculated cross sections with the experimental data of the Wisconsin group in Refs. [31,32], and also the theoretically predicted *R*-matrix values of Ref. [29]. For the $J=3$ and 2 levels, the Wisconsin group did not present any data to be compared with our predictions, but when compared to the *R*-matrix calculations we note that our cross sections are somewhat smaller near threshold for the excitation to the $J=3$ $2p_9$ level. Among the $J=2$ levels, we generally have very good agreement except very near threshold for the $2p_6$ and $2p_3$ transitions. The *R*-matrix results are somewhat larger near threshold for these two cases. For the other $J=2$ $2p_8$ level, our cross sections are larger than those given by *R*-matrix results. For the $J=0$ $2p_5$ and $2p_1$ levels, the experimental data of Ref. [31] are not definitive because of small signals, and our results are in very good agreement with the cross sections obtained by *R*-matrix calculations.

Among the four $J=1$ levels, there exist experimental data of the Wisconsin group for the $2p_4$ and $2p_2$ excitations. These data are the apparent cross sections, and, in order to compare them with our direct cross sections, the cascade contributions should be subtracted from them. It was mentioned by Piech *et al.* [31] that cascade contributions are not more than 10% in most cases. When we compare cross sections for the $2p_2$ level, we see a very reasonable agreement between our results and both the experimental data of Ref. [31] and those calculated by the *R*-matrix method. However for the $2p_4$ transition, our cross sections are much smaller except very near threshold compared to those obtained by both experiment and *R*-matrix calculations. One explanation for this could be that since this is a core-changing transition $^2P_{1/2}$-$^2P_{3/2}$ of the $3p^5$ core, our model overestimates the results. Also, the results of Ref. [31] are not corrected for the effects of cascades which become significant for certain transitions, and at higher energies it is not clear that the cascade contributions are not important for this transition. For the other two $J=1$ levels $2p_{10}$ and $2p_7$, our cross sections are much larger than those calculated by the *R*-matrix method.

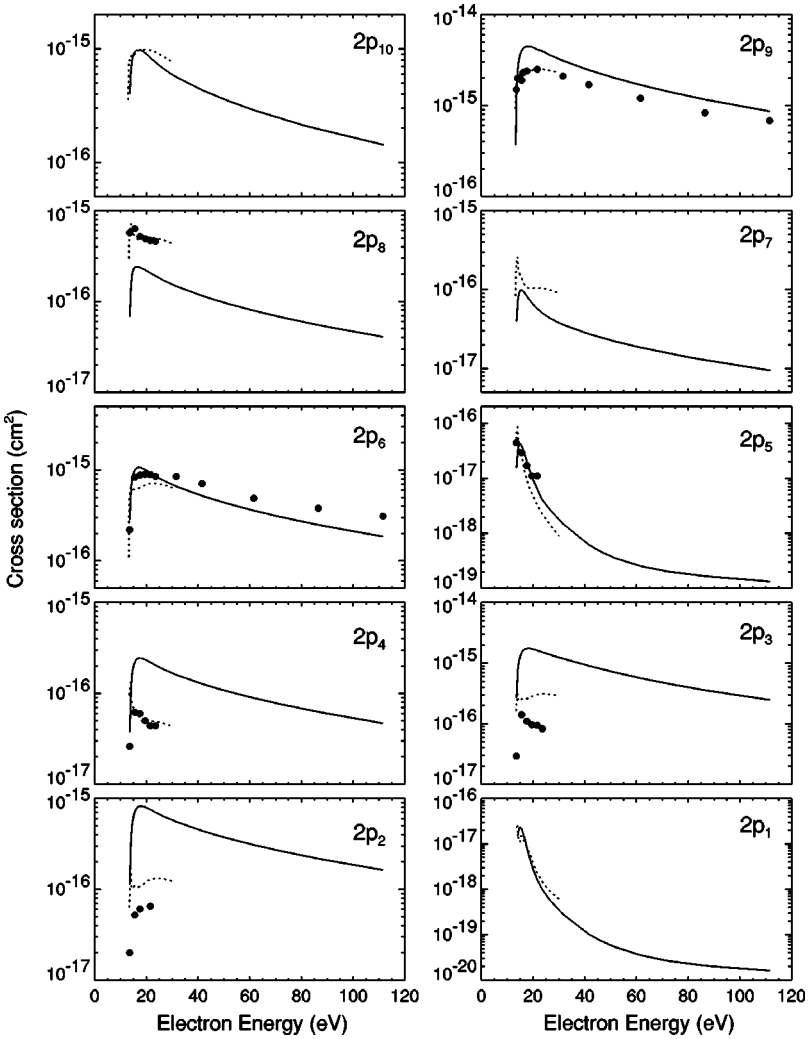

FIG. 6. Excitation cross sections from the $1s_5$ ($^3P_2$) to the $2p_1$-$2p_{10}$ excited levels of the $3p^5 4p$ configuration as a function of collision energy. The solid lines represent this calculation; dotted lines, *R* matrix (Ref. [29]); solid circles, experiment (Refs. [31] and [32]).

C. Excitation from $1s_5$ excited metastable level

We find many similarities between comparisons of our cross sections and the other available theoretical *R*-matrix calculation [29] and experimental data [31,32] for excitation from the $1s_5$ level (Fig. 6), as we found in the case of $1s_3$ excitation. Although our cross sections for excitation to the $J=3$ $2p_9$ (pure *LS* level) are larger than the Wisconsin data for lower electron energies, we found better agreement for energies above 40 eV. The *R*-matrix cross sections which are available only up to an electron energy of 30 eV are very close to the data. Of the three $J=2$ levels, we have better agreement with experiment at low collision energies than *R*-matrix calculations for the $2p_6$ excitation. However, the agreement is not so good at higher electron energies. For the $2p_8$ excitation, our cross sections are somewhat smaller, and for the $2p_3$ transition they are much larger than both Wisconsin data and *R*-matrix predictions. We could not compare our calculations at high electron collision energies for these last two transitions. The excitation cross sections for the $J=0$ $2p_5$ and $2p_1$ levels are small compared to other excitations, but for the $2p_5$ excitation our cross sections compare very well with the experimental data as well as the *R*-matrix calculations. Our cross sections also agree extremely well with the *R*-matrix calculations for the $2p_1$ excitation.

In all cases where we could compare our calculations with the experimental data of the Wisconsin group, we found the largest disagreement for $1s_5$-$2p_3$ and $1s_3$-$2p_4$ transitions. The *LS* assignment of a particular $2p_x$ level, each of which is expressed as a linear combination of states belonging to the same *J*, was done by calculating the mixing coefficients. The assignment was particularly difficult for the $2p_4$ level because the weights of $^3D_1$ and $^1P_1$ were very close. The same situation arose in the case of $2p_3$, where the contributions of both $^3P_2$ and $^1D_2$ were about the same. This may be partly responsible for the large discrepancies between our calculations and experimental data for these two particular transitions. Also, the cross sections from the $1s_5$ level to the $2p_4$ level do not agree well with either the *R*-matrix predictions or the experimental data, and thus we very much suspect that the mixing coefficients obtained for this $2p_4$ level may not be that accurate.

Finally, Fig. 7 shows comparisons of cross sections for metastable excitations obtained using the two different methods of unitarization. As shown in this graph, the cross sections for the $1s_5$-$2p_9$ excitation using the two methods are very close except for a very small energy range near the threshold of excitation. The cross sections obtained using unitarization of J^T matrices according to Eq. (4) are slightly

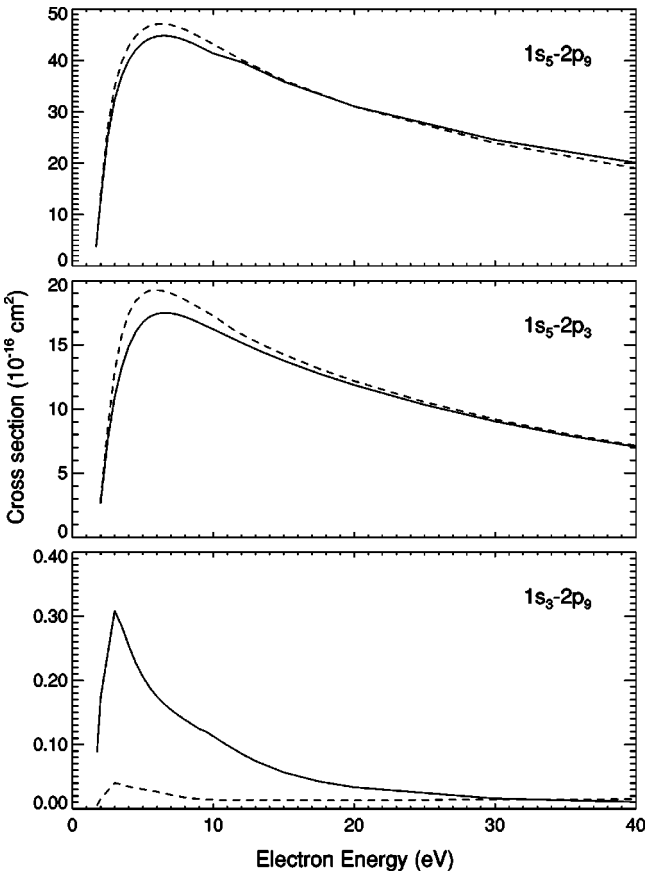

FIG. 7. Comparisons of excitation cross sections from metastable levels obtained using unitarization of the **S** matrices in LS (solid lines) and jj (dashed lines) coupling methods.

higher. For the $1s_5$-$2p_3$ excitation, the differences are more prominent although not substantial. But for the $1s_3$-$2p_9$ excitation, the results are not only very different, the cross sections obtained using the unitarization of $S^T L^T$ matrices (in the LS formalism) are much higher than those obtained using the other method. For this transition, where $\Delta J=3$, the unitarization of the J^T matrices does not produce accurate results. This can be explained by the fact that for this case where exchange is dominant implying close collision, electrostatic interaction is much stronger than spin-orbit interaction, and hence unitarization in the LS formalism seems more appropriate. Unitarization of the **S** matrices by either of these two methods reduces the cross sections significantly. The cross sections obtained using unitarization in the LS formalism for the $1s_5$-$2p_9$ transition around the peak, for example, are about 50% smaller than those calculated using no unitarization.

IV. SUMMARY

The DW method is expected to give reliable results at high electron collision energies. Since it is well known that *R*-matrix results generally are better than DW results at energies near the threshold of excitation, and usually are not as accurate as DW calculations as the energy increases, these two methods can complement each other over a long range of energy. Although in our method we used first-order perturbation theory, we have used the final-state potential for incoming and outgoing channels in contrast to the usual use of initial-state interaction in any fist-order many-body calculation. We have neglected any relativistic effects, contrary to the RDW and SRDW calculations of Refs. [15] and [14], respectively. However we do not expect relativity to play an important role for an atom such as argon. We have used specific fine-structure level energy in order to calculate the radial wave function for each J level belonging to a given LS configuration, whereas in the RDW method of Ref. [15] all the fine-structure levels belonging to a particular LS have the same energy. We have calculated and included a polarization potential, but its effect is not found to be significant. However, unitarization of the $S^T L^T$ or J^T matrices does have significant effects on the cross sections.

To summarize the comparison of our cross sections for ground-state excitation, the close agreement, between our results for all the levels in the $1s$ manifold and with most of the levels in the $2p$ manifold, with the *R*-matrix results at low energies and with the SRDW results of Ref. [14] at higher energies, is very encouraging. Unfortunately we do not have such agreement with the experimental data of the Wisconsin group in many transitions, especially for the $J=1$ $3p^5 4p$ levels at high energies. Inclusion of second-order transitions with two direct components may improve our cross sections and bring them into close agreement with measurements. On the other hand, the extremely slow falloff of the Wisconsin data for these transitions is suspicious, and hence further improvements of experimental investigation must be considered for this difficult problem of collision excitations of neutral rare gases. The results of our calculations for excitation from the metastable $1s_3$ and $1s_5$ levels could only be compared for low energies with *R*-matrix calculations, and we have close agreement in about half of the cases. At higher energies we could compare our results with the experimental data of the Wisconsin group only for the $1s_3$-$2p_4$, $1s_5$-$2p_6$, and $1s_5$-$2p_9$ transitions, and except for the $1s_3$-$2p_4$ transition our results agree well for the other two cases. As mentioned previously, since the data are for apparent cross sections and do not include any cascade corrections, the direct cross sections are actually lower, which will make the disagreement somewhat smaller.

In addition to inclusion of secondary effects, another improvement on the calculation would be to obtain more accurate bound wave functions and hence more accurate mixing coefficients for the mixed levels. In the inner region, where it is important to obtain the bound functions accurately, one should try to improve these wave functions by including configuration interactions of levels of same parity and by checking the convergences of the atomic parameters, and comparing them with experimental values. A close-coupling (CC) calculation with a basis of many states is superior to a Hartree-Fock calculation to generate these wave functions. Indeed, if we use wave functions generated by a CC approximation such as the *R*-matrix method, we will have better agreement with experimental measurements, especially at low electron energies; however, in this work both the atomic

structure and the collision calculations are done self-consistently. When comparison is made with the *R*-matrix results, this work shows the limitations of using a DW method to calculate near-threshold excitation of neutral atoms precisely. However, over a large energy range the present DW method with proper unitarization gives acceptable results for many excitation cross sections.

ACKNOWLEDGMENTS

We would like to thank Dr. K. Bartschat for allowing us to present some of his results before publication. A.D. would also like to thank K. Bartschat and D. H. Madison for useful discussions during the course of this work. This work was supported by BMDO and the Office of Naval Research.

[1] J. W. Coburn and M. Chen, J. Appl. Phys. **51**, 3134 (1980).
[2] S. E. Savas, Appl. Phys. Lett. **48**, 1042 (1986).
[3] M. V. Malyshev and V. M. Donnelly, J. Vac. Sci. Technol. A **15**, 550 (1997).
[4] F. J. Grunthaner, R. Bicknell-Tassius, P. Deelman, P. J. Grunthaner, C. Bryson, E. Snyder, J. L. Giuliani, J. P. Apruzese, and P. Kepple, J. Vac. Sci. Technol. A **16**, 1615 (1998).
[5] J. D. Sethian, S. P. Obenschain, K. A. Gerber, C. J. Pawley, V. Serlin, C. A. Sullivan, W. Webster, A. V. Deniz, T. Lehecka, M. W. McGeoch, R. A. Altes, P. A. Corcoran, I. D. Smith, and O. C. Barr, Rev. Sci. Instrum. **68**, 2357 (1997).
[6] A. E. Mandel, D. E. Klimek, and E. T. Salesky, Fusion Technol. **11**, 542 (1987).
[7] L. R. Peterson and J. E. Allen, J. Chem. Phys. **56**, 6068 (1972).
[8] F. Kannari, M. Obara, and T. Fujioka, J. Appl. Phys. **57**, 4309 (1985).
[9] T. Swada, J. E. Purcell, and A. E. Green, Phys. Rev. A **4**, 193 (1971).
[10] N. T. Padial, G. D. Meneses, F. J. da Paixao, G. Csanak, and D. C. Cartwright, Phys. Rev. A **23**, 2194 (1981).
[11] K. Bartschat and D. H. Madison, J. Phys. B **20**, 5839 (1987).
[12] S. Wang, P. J. M. van der Burgt, J. J. Corr, J. W. McConkey, and D. H. Madison, J. Phys. B **27**, 329 (1993).
[13] D. C. Griffin, M. S. Pindzola, T. W. Gorczyca, and N. R. Badnell, Phys. Rev. A **51**, 2265 (1995).
[14] D. H. Madison, C. M. Maloney, and J. B. Wang, J. Phys. B **31**, 873 (1998).
[15] S. Kaur, R. Srivastava, R. P. McEachran, and A. D. Stauffer, J. Phys. B **31**, 4833 (1998).
[16] A. Chutjian and D. C. Cartwright, Phys. Rev. A **23**, 2178 (1981).
[17] M. A. Khakoo, C. E. Beckmann, S. Trajmar, and G. Csanak, J. Phys. B **27**, 3159 (1994).
[18] R. S. Schappe, M. B. Schulman, L. W. Anderson, and C. C. Lin, Phys. Rev. A **50**, 444 (1994).
[19] S. Tsurubuchi, T. Miyazaki, and K. Motohashi, J. Phys. B **29**, 1785 (1996).
[20] R. Albat, N. Gruen, and B. Wirsam, J. Phys. B **8**, L82 (1975).
[21] V. E. Bubelev and A. N. Grum-Grzhimailo, J. Phys. B **24**, 2183 (1991).
[22] S. S. Tayal and R. J. W. Henry, J. Phys. B **29**, 3443 (1996).
[23] J. K. Ballou, C. C. Lin, and F. E. Fajen, Phys. Rev. A **8**, 1797 (1973).
[24] I. P. Bogdanova and S. V. Yurgenson, Opt. Spectrosk. **62**, 471 (1987) [Opt. Spectrosc. **62**, 281 (1987)].
[25] T. J. Gay, J. E. Furst, K. W. Trantham, and W. M. K. P. Wijayaratna, Phys. Rev. A **53**, 1623 (1996).
[26] J. E. Chilton, J. B. Boffard, R. S. Schappe, and C. C. Lin, Phys. Rev. A **57**, 267 (1998).
[27] K. Bartschat and V. Zeman (private communication).
[28] H. A. Hyman, Phys. Rev. A **24**, 1094 (1981).
[29] K. Bartschat and V. Zeman, Phys. Rev. A **59**, R2552 (1999).
[30] J. B. Boffard, G. A. Piech, M. F. Gehrke, and M. E. Lagus, J. Phys. B **29**, L795 (1996).
[31] G. A. Piech, J. B. Boffard, M. F. Gehrke, L. W. Anderson, and C. C. Lin, Phys. Rev. Lett. **81**, 309 (1998).
[32] J. B. Boffard, G. A. Piech, M. F. Gehrke, L. W. Anderson, and C. C. Lin, Phys. Rev. A **59**, 2749 (1999).
[33] I. Yu. Baranov, N. B. Kolokolov, and N. P. Penkin, Opt. Spektrosk. **58**, 268 (1985) [Opt. Spectrosc. **58**, 160 (1985)]; A. A. Mityureva, N. P. Penkin, and V. V. Smirnov, *ibid.* **66**, 790 (1989) [*ibid.* **66**, 463 (1989)].
[34] E. Clementi, IBM J. Res. Dev. **9**, 2 (1965).
[35] M. Blaha and J. Davis, J. Quant. Spectrosc. Radiat. Transf. **19**, 227 (1978).
[36] A. Dasgupta and A. K. Bhatia, Phys. Rev. A **32**, 3335 (1985).
[37] M. J. Seaton, Proc. Phys. Soc. London **77**, 174 (1961).
[38] A. Dasgupta, K. G. Whitney, M. Blaha, and M. Buie, Phys. Rev. A **46**, 5973 (1992).